Journal of Molecular Graphics and Modelling 41 (2013) 43–54

Contents lists available at SciVerse ScienceDirect

Journal of Molecular Graphics and Modelling

journal homepage: www.elsevier.com/locate/JMGM

Synthesis and evaluation of resveratrol derivatives as new chemical entities for cancer

Chaitanya Mulakayala[a], B. Babajan[a], P. Madhusudana[a], C.M. Anuradha[b], Raja Mohan Rao[c], Ravi Prakash Nune[d], Sunil Kumar Manna[d], Naveen Mulakayala[c], Chitta Suresh Kumar[a,*]

[a] Department of Biochemistry, Sri Krishandevaraya University, Anantapur 515003, A.P., India
[b] Department of Biotechnology, Sri Krishandevaraya University, Anantapur 515003, A.P., India
[c] Institute of Life Sciences, University of Hyderabad Campus, Gachibowli, Hyderabad 500046, India
[d] Laboratory of Immunology, Center for DNA finger Printing and Diagnosis, Nampally, Hyderabad 500001, India

ARTICLE INFO

Article history:
Accepted 17 January 2013
Available online 4 February 2013

Keywords:
EMSA
TNFα
FasL
MTT
TNF
NF-kB
Docking
Dynamics

ABSTRACT

Resveratrol has been shown to be active in inhibiting multistage carcinogenesis. The potential use of resveratrol in cancer chemoprevention or chemotherapy settings has been hindered by its short half-life and low bioavailability. Considering the above remarks, using resveratrol as a prototype, we have synthesized two derivatives of resveratrol. Their activity was evaluated using in vitro and in silico analysis. Biological evaluation of resveratrol analogues on U937 cells had shown that two synthesized analogues of resveratrol had higher rates of inhibition than the parental molecule at 10 μM concentration. EMSA conducted for NF-kB revealed that these molecules significantly interfered in the DNA binding ability of NF-kB. It was found that these molecules suppressed the expression of TNFα, TNFR, IL-8, actin and activated the expression of FasL, FasR genes. To understand possible molecular mechanism of the action we performed docking and dynamic studies, using NF-kB as a receptor. Results showed that resveratrol, RA1 and RA2 interacted with the residues involved in DNA binding. Resveratrol analogues by interacting NF-kB might have prevented its translocation and also by interacting with the residues involved in DNA binding might have prevented the binding of NF-kB to DNA. This may be the reason for suppression of NF-kB binding to DNA.

1. Introduction

Epidemiological and animal studies have demonstrated that plant-derived dietary constituents of food play an important role in the prevention of disease [1,2]. A number of food components that inhibit the initiation and progression of cancer or otherwise influence the potential for disease outcome have been identified [3–5]. The beneficial effects of these dietary compounds have been attributed partly to the presence of numerous polyphenolic compounds with antioxidant and free radical scavenging properties [6,7]. This conclusion is best supported by epidemiological studies showing a close association between low incidence of various forms of cancer by the consumption of diet containing natural polyphenolic compounds that have potent antitumor-promoting activities combined with low toxicity and very few adverse side effects [8].

Resveratrol (3,5,4′-trihydroxystilbene) is a member of the phytoalexin class of antibiotics and is induced in a variety of plants in response to fungal infection, environmental stress, or injury. Resveratrol is a well-known component of the skin of grapes, is present in high concentrations in red wine, and is also found in other fruits such as blueberries, mulberries, rhubarb, and cranberries [9]. Resveratrol has been shown to exert chemopreventive effects against cancer based on its inhibition of cellular events associated with tumor initiation, promotion and progression in both cell culture and animal models [10–12]. Resveratrol was found to interfere in the nuclear factor (NF)-kB signaling pathway, which regulates the expression of various genes involved in cancer and inflammation [13,14]. Recently, it was found that the cancer chemopreventive activity of resveratrol was related to its ability to trigger apoptosis [15–17].

In view of the great potential of resveratrol as a potent chemotherapeutic agent against a wide variety of cancers, the trihydroxystilbene scaffold of resveratrol has been subjected to synthetic manipulations with the aim of generating novel resveratrol derivatives with improved anti-cancer activity. In this study, we aimed to assess and compare the anti-tumor effects of resveratrol derivatives using U937 cancer cell line. The tested derivatives

* Corresponding author at: Department of Biochemistry, Bioinformatics Infrastructure Facility (BIF), Sri Krishnadevaraya University, Anantapur 515003, Andhrapradesh, India. Tel.: +91 8554 255466; fax: +91 8554 255466.
E-mail address: chitta34c@gmail.com (C.S. Kumar).

1093-3263/$ – see front matter © 2013 Elsevier Inc. All rights reserved.
http://dx.doi.org/10.1016/j.jmgm.2013.01.005

were shown to possess stronger anti-proliferative properties than resveratrol in U937 cancer cells. In addition, the synthesized derivatives were found to preferentially inhibit the growth of cancer cells. It has been documented that interference of NF-kB transcription is the cause for inducing apoptosis in transformed cells. In addition it has been found that the resveratrol derivatives induced PARP cleavage in the transformed cells. In order to further investigate the structural details of the interactions between NF-kB and synthesized resveratrol derivatives at molecular level, we performed docking studies using AutoDock 4.2. The stabilities of the docked complexes were determined using molecular dynamic studies with Gromacs 4.0.5. The stabilized complexes were further docked onto DNA binding site of NF-kB using HEX server to predict the molecular basis for inhibition of DNA binding by NF-kB ligand complex. These features should make the synthesized resveratrol derivatives as interesting compounds for further evaluation as potential chemopreventive and chemotherapeutic agents.

2. Materials and methods

2.1. Materials

2.1.1. Biological work

Resveratrol, propidium iodide (PI), MTT, DMSO were purchased from Sigma–Aldrich Chemicals (St. Louis, MO, USA). Penicillin, streptomycin, neomycin, RPMI 1640, Fetal Bovine Serum (FBS), were obtained from Life Technologies (Grand Island, NY, USA). Antibodies against PARP and gel shift oligonucleotides for NF-kB were purchased from Santa Cruz Biotechnology, Inc. (Santa Cruz, CA, USA).

2.1.1.1. Cell lines. The cell line used in this study was U937 (human histiocytic lymphoma) obtained from American Type culture collection (Manassas, VA, USA). Cells were maintained in RPMI 1640 supplemented with penicillin, streptomycin (1%) and heat-inactivated FBS (10%). Cells were grown at 37 °C in a 5% CO_2 humidified incubator.

2.1.2. In silico work

2.1.2.1. Hardware. Docking and dynamics studies were performed using a quadracore AMD platform, run on a Linux operating system with a, 6 GB RAM.

2.1.2.2. Software. All automated docking simulations of protein and ligands were performed with AutoDock 4.2 and molecular dynamics simulations were performed with Gromacs 4.0.5. Docking of DNA with complexes of protein and ligand was done by HEX server.

2.2. Synthesis of resveratrol derivatives

Resveratrol derivatives were synthesized by adding a mixture of resveratrol (SIGMA, 99% purity; 100 mg, 1 eq) and K_2CO_3 (2 eq) in dry acetone (4.0 ml) and to this allyl bromide was added 3 eq) and heated to reflux. After completion of starting material (TLC monitoring) the reaction mixture was evaporated and the crude product was purified using column chromatography by eluting with chloroform–MeOH (10/1) as elutent. In this process, (E)-1,3-bis(allyloxy)-5-(4-(allyloxy) styryl) benzene (RA1) and (E)-3-(allyloxy)-5-(4-(allyloxy) styryl) phenol benzene (RA2) were obtained as a colorless amorphous powder. The two resveratrol derivatives obtained by this procedure are given the names RA1 and RA2. Resveratrol, RA1 and RA2 were subjected to Molinspiration server to determine their ability to obey Lipinski rule-of-five [18] for drug likeliness.

2.3. Biological evaluation

Resveratrol and its synthesized derivatives RA1 and RA2 were subjected to biological evaluation using U937 cell lines.

2.3.1. Cytotoxicity assays

Resveratrol, RA1 and RA2 were subjected to cytotoxicity assays using tetrazolium salt 3-(4,5-dimethylthiazol-2-yl)-2,5-diphenyltetrazolium bromide (MTT) method [19]. Briefly 10^4 cells/well of a 96-well plate were incubated with the resveratrol and its derivatives RA1 and RA2 in separate wells at different concentrations (1 μM, 3 μM, 5 μM and 10 μM) for 72 h at 37 °C. Thereafter, the cell viability was determined by incubating the cells with the 25 μl MTT dye (5 mg/ml in PBS) for 4 h at 37 °C. The cells were incubated with 100 μl lysis buffer (20% SDS in 50% dimethylformamide) for overnight at 37 °C, and the absorbance was read at 570 nm.

2.3.2. Determination of nuclear fragmentation by PI staining

The process of apoptosis was identified through nuclear fragmentation by propidium iodide (PI) staining. U937 cells were treated with RA1, RA2 and resveratrol at 10 μM concentration for 48 h. After the incubation period of 48 h the cells were harvested and fixed in 80% methanol, stained with PI, and viewed under fluorescence microscope [20].

2.3.3. DNA fragmentation assay

This procedure is based on internucleosomal DNA cleavage, a characteristic biochemical hallmark of the apoptotic mode of cell death [21]. DNA was extracted from resveratrol and its derivatives (RA1 and RA2) treated U937 cells by suspending the cell pellet in 20 μl of lysis buffer (10 mM EDTA, 50 mM Tris at pH 8.0 and 0.5%, w/v, SDS) containing proteinase K. The whole lysate was incubated at 50 °C for 1 h in water bath. After the completion of incubation, to the condensate 10 μl of RNase was added and further incubated for 1 h at 50 °C in water bath. This was centrifuged for 15 s and ran on 1% agarose gel. DNA fragments were visualized as ladder with ethidium bromide under UV light.

2.3.4. Western blot of PARP

Apoptosis was confirmed by proteolytic cleavage of PARP. The cells were treated with resveratrol and its derivatives (RA1 and RA2) at 10 μM concentration for 72 h at 37 °C. After treatment, cell extracts were prepared by incubating the cells for 30 min on ice in 0.05 ml of buffer containing 20 mM HEPES, pH 7.4, 2 mM EDTA, 250 mM NaCl, 0.1% Nonidet P-40, 2 μg/ml aprotinin, 1 mM phenylmethylsulfonyl fluoride, 0.5 μg/ml benzamidine and 1 mM dithiothreitol. The lysate was centrifuged and the supernatant was collected. Cell extract protein (40 μg) was resolved in 10% SDS-polyacrylamide gel electrophoresis. Then it was electrotransferred onto a nitrocellulose membrane, blotted with mouse anti-PARP antibody, and then detected by chemiluminescence (ECL; Amersham Pharmacia Biotech). Apoptosis was represented by the cleavage of 116 kDa PARP into an 89 kDa peptide product.

2.3.5. Electrophoretic mobility shift assay (EMSA) for NF-kB

U937 cells treated with resveratrol and its derivatives at 10 μM concentration and nuclear extracts were prepared and assayed for NF-kB activation using EMSA [22]. Cells were suspended in 0.4 ml of lysis buffer (10 mM HEPES, pH 7.9), 10 mM KCl, 0.1 mM EDTA, 0.1 mM EGTA, 1 mM DTT, 0.5 mM PMSF, 2 μg/ml leupeptin and 2 μg/ml aprotinin and incubated on ice for 15 min, after which 12.5 μl of 10% Nonidet P-40 was added. The tube was then vigorously shaken on a vortex machine for 10 s, and the homogenate was centrifuged at maximum speed for 30 s in a microfuge [22]. The

nuclear pellet was re-suspended in 25 μl of ice cold nuclear extraction buffer (20 mM HEPES (pH 7.9), 0.4 M NaCl, 1 mM EDTA, 1 mM EGTA, 1 mM DTT, 1 mM PMSF, 2.0 μg/ml leupeptin and 2.0 μg/ml aprotinin). The tube was incubated on ice for 30 min with intermittent mixing and finally centrifuged for 5 min in a microfuge at 4 °C, and the supernatant (nuclear extract) was collected. 8 μg of nuclear extract was incubated in a mixture containing 2 μg of poly dI:dC in a binding buffer (25 mM HEPES, pH 7.9, 0.5 mM EDTA, 0.5 mM DTT, 1% Nonidet P-40, 5% glycerol, and 50 mM NaCl) with double-stranded NF-kB oligonucleotide of HIV-LTR, 5′-TTG TTA CAA **GGG ACT TT**C CGC TG**G GGA CTT T**CC AGG GAG GGG TGG-3′ (bold indicates NF-kB binding site) for 30 min at 37 °C, and the DNA–protein complex formed was separated from free oligonucleotide on 6.6% native polyacrylamide gels. The gel was dried and exposed in a phosphor screen and scanned in a PhosphorImager (Fuji Photo Film, Japan) [23].

2.3.6. Measurement of NF-kB dependent genes by semi-quantitative RT-PCR

To determine the levels of expression of IL-8, TNFα, TNFR, FasL, FasR and actin we performed RT-PCR for this, U937 cells were treated with 10 μM concentration of resveratrol and its derivatives RA1 and RA2 for 72 h and total RNA was isolated using the standard Trizol method (Gibco BRL). One microgram of total RNA was used to reverse transcribe into cDNA. One step Access RT-PCR kit (Promega) was used for the synthesis of cDNA followed by the amplification of the gene of interest using gene specific primers. Amplification products were separated by agarose gel electrophoresis and visualized by Ethidium bromide staining. The primer sequences used were as follows:

IL-8: 5′-GCAGCTCTGTGTGAAGGTGCA-3′ {forward};
5′-CAGACAGAGCTCTCTTCCAT-3′ {reverse};
Actin: 5′-AGCGAGCATCCCGCAAAGTT-3′ {forward};
5′-GGGCACGAAGGCTCATCATT-3′ {reverse};
TNFR: 5′-CGCTTCAGAAAACCACCTCAGAC-3′ {forward};
5′-CCAAAGAAAATGACCAGGGGC-3′ {reverse};
TNFα: 5′-GCGAGCATCCCCCAAAGTT-3′ {forward};
5′-GGGCACGAAGGCTCATCATT3′ {reverse};
FASL: 5′-CCAACCGTGAAAGTT3′ {forward};
5′-GCAGTAATCTCCTTCTGCATC-3′ {reverse};
FASR: 5′-TGGCTTTTCTTCTTCTTTTG-3′ {forward};
5′-TCATCTATTTTGGCTTCATTG-3′ {reverse};

2.4. In silico analysis

The ability of resveratrol as well as its derivatives RA1 and RA2 to exert antiproliferative effects by inducing apoptosis and by interfering in the binding of NF-kB to DNA made us to study the possible mode of action of resveratrol and its synthesized derivatives RA1 and RA2 on NF-kB protein at molecular level. For this purpose we conducted docking analyses of the tested resveratrol derivatives (RA1 and RA2) onto NF-kB and the stability of the complex was determined by dynamic simulations. The stabilized complex was further docked onto the DNA binding site of NF-kB.

2.4.1. Structure preparation

The crystallographic coordinates of the NF-kB protein along with its DNA binding domain were obtained from RCSB Protein Data Bank with PDB ID: 3GUT [24]. All crystallographic water molecules were removed from the crystal structure. Coordinates of the DNA binding domain were removed and saved for further use of docking with the complex. From the PDB file of 3GUT chain A (p65) and chain B (p50) were retained and rest of the chains were removed. This NF-kB protein was minimized by subjecting to molecular dynamic (MD) simulations using the GROMACS 4.0.5 [25] package with GROMOS96 [26] 43a1 force field implemented on a LINUX architecture. The starting structure was immersed in a dodecahedron of SPC water molecules [27]. To neutralize the charge of the system 24CL^- ions were added. The system was subjected to energy minimization for 2000 steps by steepest descents. The equilibrated systems were then subjected to molecular dynamics simulations for 10 ns. Periodic boundary conditions were used under isothermal, isobaric conditions using Berendsen coupling algorithm [28]. The LINCS algorithm [29] was used to constrain bond lengths using a time step of 2 fs for all calculations. Electrostatic interactions were calculated using the Particle Mesh Ewald (PME) [30] summation scheme. Van der Waals and Coulomb interactions were truncated at 0.9 nm. The non-bonded pair list was updated for every 10 steps and conformations were stored for every 2 ps.

2.4.2. Docking studies of resveratrol and its derivatives onto NF-kB protein

The ability of resveratrol and its derivatives (RA1 and RA2,) to decrease the transcription of NF-kB made us to understand the binding modes of these compounds at molecular level onto NF-kB. The goal was to evaluate the binding orientations, and conformations of resveratrol and its derivatives onto NF-kB, and to study the key ligand-receptor interactions involved in the molecular recognition process. The 3D structures of the resveratrol and its derivatives RA1 and RA2 were generated by PRODRG [31] and preoptimized using the MMFF94x force field. Each compound was docked into the minimized, structure of NF-kB using AutoDock4.2 software package from The Scripps Research Institute [32]. The files for docking calculations were prepared using AutoDock Tools (ADT) [33]. AutoDock uses a rapid grid-based method for energy evaluation. For all docking calculations the size of the grid was set to 80 Å × 80 Å × 80 Å using grid spaces between 1.0. For the docking protocol, three built-in algorithms of Autodock4, Lamarckian Genetic Algorithm (LGA) [34,35], Genetic Algorithm (GA) [36], and Simulated Annealing (SA) [37] were probed in order to find the most favorable ligand–protein complex geometry or in other words the most favorable interactions. The LGA algorithm predicted the strongest ligand–receptor affinity in all cases, and therefore, throughout this study, the LGA-computed expected binding energies were used. For all the simulations, the docking runs were set to 100. For GA and LGA searching algorithms the number of energy evaluations was set to 25,000,000 while the population was set to 300. The other docking parameters were set to the default values for all three algorithms.

2.4.3. Molecular dynamic (MD) simulations of the complexes

Four independent MD simulations were carried out for the four different models (NF-kB alone, NF-kB-resveratrol, NF-kB-RA1 and NF-kB-RA2) complexes produced by AutoDock with the program package GROMACS v.4.0.5 [25], using the GROMACS96 (43A1) force field [26], the SPC water model [27] and the leap-frog integration scheme. Before the MD simulations, an energy minimization procedure was split into three steps. First, an energy minimization using the steepest-descent algorithm was made, allowing the solvent to relax while restraining the protein and ligand heavy atoms to their original positions with a harmonic potential. Then, another minimization using steepest-descent with no restraints was performed, allowing relaxation of the entire system. Finally, an energy minimization procedure with all restraints already removed was conducted, using the conjugate gradient method. After the minimization process, two stages of equilibration were conducted: a 500 ps MD simulations with protein non-hydrogen atoms positions restrained to allow the formation of solvation layers and another of 2 ns without positional restriction. This second step is important for the system to accommodate the thermodynamic conditions imposed in the simulation. After those equilibration stages, an MD simulation of 10 ns was conducted for further analysis.

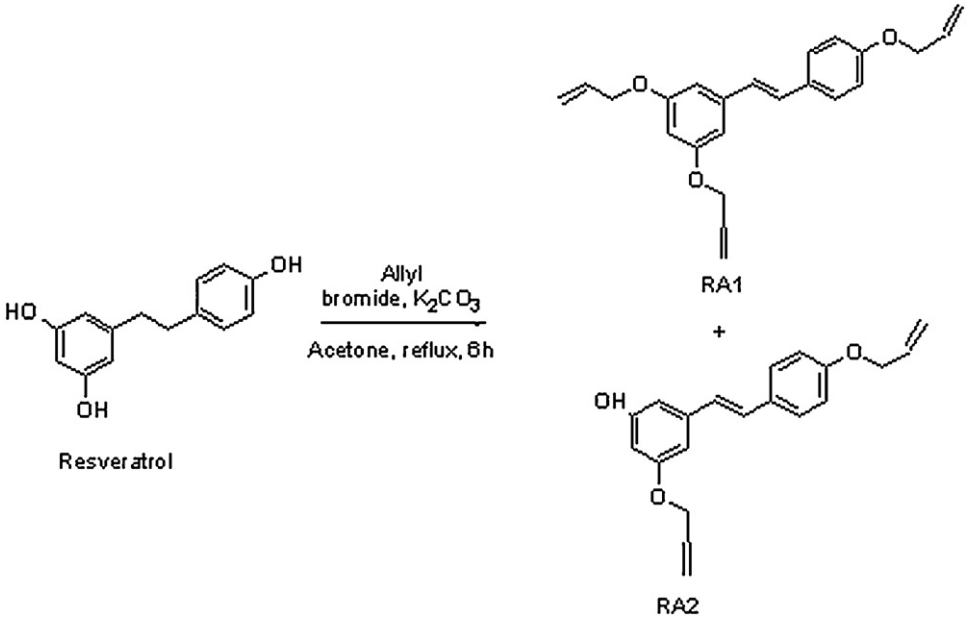

Fig. 1. Schematic representation of the synthesis of resveratrol derivatives RA1 and RA2.

All MD simulations applied the constraint algorithms SETTLE [38] and LINCS [29]. The LINCS algorithm was used to constrain all the covalent bonds in non-water molecules, while the SETTLE algorithm was used to constrain bond lengths and angles in water molecules. The temperature was maintained at 300 K and the pressure at 1 atm by using Berendsen weak coupling approach [28]. For Coulomb interactions, the reaction field correction term [39] was employed, with a dielectric constant set to 54 [40]. Cutoff values of 1.6 Å and 1.8 Å were used for van der Waals and Coulomb interactions, respectively. All molecular structures were inspected using the programs VMD [41] and Pymol [42].

2.4.4. Docking of complexes with DNA

To better understand the mechanism of interference of DNA binding by NF-kB-resveratrol, NF-kB-RA1 and NF-kB-RA2 complexes, docking was performed using HEX server [43]. PDB structure of the double stranded DNA (3GUT) possessing a length of 26 bps, acting as binding domain for NF-kB was used as DNA for docking experiments with the complexes. Four independent docking experiments were performed with NF-kB alone, with NF-kB-resveratrol, with NF-kB-RA1 and with NF-kB-RA2. During docking Hex adjusts the position of DNA by initial alignment over the proposed binding sites. For employing the steric and electrostatic interactions between the complex of protein and ligand with DNA a pre-computing box region was employed by HEX. This program allows the selection of H-bonding interactions between the residues of protein in the pocket with that of ligand and to that of DNA. During docking no rotational bonds in the DNA back bone were selected. The obtained docking results were analyzed by energy total obtained during docking and using RMSD of superposition of each of the docked complexes of NF-kB-resveratrol-DNA and its derivatives NF-kB-RA1-DNA and NF-kB-RA2-DNA onto NF-kB-DNA complex.

3. Results and discussion

3.1. Synthesis of resveratrol derivatives

Fig. 1 shows schematic representation of the synthesis of resveratrol derivatives: (E)-1,3-bis(allyloxy)-5-(4-(allyloxy)styryl) benzene (RA1) and (E)-3-(allyloxy)-5-(4-(allyloxy) styryl) phenol benzene (RA2). ^{1}H NMR spectra for RA1 is (400 MHz, *CDCl$_3$*) ppm 4.61–4.50 (m, 6H), 5.30 (d, *J* = 10.49 Hz, 3H), 5.43 (d, *J* = 17.25 Hz, 3H), 6.18–5.98 (m, 3H), 6.41 (s, 1H), 6.66 (d, *J* = 2.05 Hz, 2H), 6.89 (dd, *J* = 12.18, 10.95 Hz, 3H), 7.01 (d, *J* = 16.24 Hz, 1H), 7.43 (d, *J* = 8.70 Hz, 2H) and for RA2 (400 MHz, *CDCl$_3$*) ppm 4.55 (dd, *J* = 6.51, 5.47 Hz, 4H), 5.30 (d, *J* = 10.51 Hz, 2H), 5.42 (dd, *J* = 17.26, 1.36 Hz, 2H), 6.06 (dtd, *J* = 6.27, 5.21, 2.52 Hz, 2H), 6.36–6.31 (m, 1H), 6.57 (s, 1H), 6.64 (s, 1H), 6.94–6.81 (m, 3H), 7.00 (dd, *J* = 16.21, 4.55 Hz, 1H), 7.40 (t, *J* = 8.41 Hz, 2H). The two synthesized compounds were analyzed for their drug-likeliness based on their physiochemical properties using Lipinski rule-of-five by Molinspiration server (Table 1) and both were found to obey Lipinski's rule this supports their drug-likeliness.

3.2. Biological evaluation

The synthesized derivatives of resveratrol were evaluated for their antitumorigenic activities through in vitro evaluation using U937 cell lines.

3.2.1. Cell viability assay

To determine the cytotoxic effects of synthesized resveratrol derivatives, we incubated U937 cells with different concentrations (1 μM, 3 μM, 5 μM and 10 μM) of RA1, RA2, and resveratrol for 72 h and cell viability was assayed using MTT dye. 40–50% of cell death was observed in RA1 and RA2 treated cells at 10 μM concentration whereas 15% of cell death was seen with resveratrol treated cells at 10 μM concentration (Fig. 2). Among the three compounds, RA1 has shown highest percentage of cell death at 10 μM concentration and it was shown to be three times more than that of resveratrol (Fig. 2). The IC_{50} values calculated for resveratrol, RA1 and RA2 are 32.01 μM, 10.372 μM and 13.372 μM. Previously Minutolo et al. [44] and Simoni et al. [45] demonstrated that treatment with methoxy resveratrol derivatives, yielded higher cytotoxicity than resveratrol in MDA-MB-231 and HL-60 cells. As mentioned in Minutolo et al. [44] and Simoni et al. [45] work, due to capping of hydroxyl groups for methoxy derivatives the bioavailability got increased. Resveratrol derivatives RA1 and RA2, might have displayed higher pharmaceutical activity and bioavailability than

Table 1
Physicochemical properties obtained for resveratrol and its derivatives RA1 and RA2 calculated using Molinspiration.

Compound	Log *P*	TPSA	*n* atoms	MW	*n* ON	*n* OHNH	*n* violations	*n* rotate	Volume
Resveratrol	2.786	60.684	17	228.247	3	3	0	2	206.922
RA1	4.963	27.702	26	348.442	3	0	0	3	341.756
RA2	4.682	38.696	23	308.377	3	1	0	6	296.282

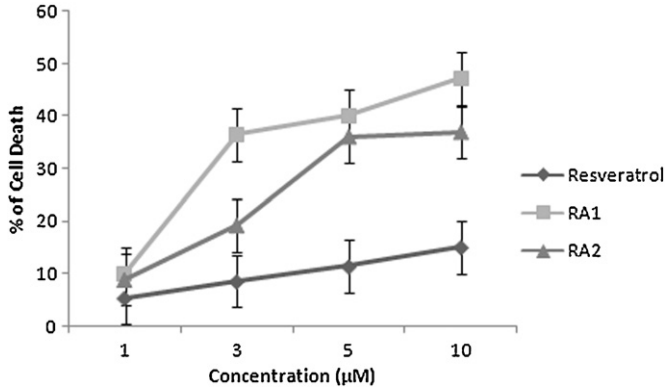

Fig. 2. Cell viability by MTT assay in U937 cells. Dose dependent effect of resveratrol and its derivatives RA1 and RA2 on U937 cell lines. Cells (1×10^6 cells/ml) were incubated with different concentrations of resveratrol and its derivatives for 72 h. The cytotoxic index was determined using MTT assay.

the parental molecule resveratrol, due to the capping of hydroxyl groups.

3.2.2. *Resveratrol and its derivatives induces nuclear fragmentation in U937 cells*

U937 cells were treated with resveratrol and its derivatives for 72 h at a concentration of 10 μM and the extent of apoptosis was assessed by PI staining. All the treated cells contained more apoptotic cells whereas in untreated cells apoptosis is almost absent. There was characteristic nuclear fragmentation of nuclei in treated cells whereas the untreated control cells did not show such kinds of fragmentation (Fig. 3). Among all the treated cells RA1 has shown to induce more number of nuclear fragmentations (Fig. 3). The apoptotic cells displayed the characteristic features of reduced size, intense fluorescence of condensed nuclear chromatin and formation of membrane blebs (Fig. 3). PI staining results showed that resveratrol and its derivatives RA1 and RA2 induced the death of cancerous cells through apoptosis. This can be due to increase in bioavailability and halflife period of resveratrol and its derivatives. The increase in apoptosis inducing capacity of resveratrol derivatives than resveratrol, might be due to increase in bioavailability and is due to capping of its hydroxyl groups. This capping might have decreased the easily excretion of these compounds thereby the half life periods might have got increased [46,47].

3.2.3. *Resveratrol and its derivatives induces DNA fragmentation in U937 cells*

To further characterize resveratrol and its derivatives induced cell death is apoptosis or the other mode of cell death, we performed DNA fragmentation analysis. Gel electrophoresis was performed with the isolated DNA, in order to confirm whether the pattern of DNA fragmentation is the typical apoptotic "DNA ladder" or not. As shown in Fig. 4, resveratrol and its analogues RA1 and RA2 treated U937 cells showed DNA ladder formation whereas DNA fragmentation is completely absent in the DNA isolated from untreated

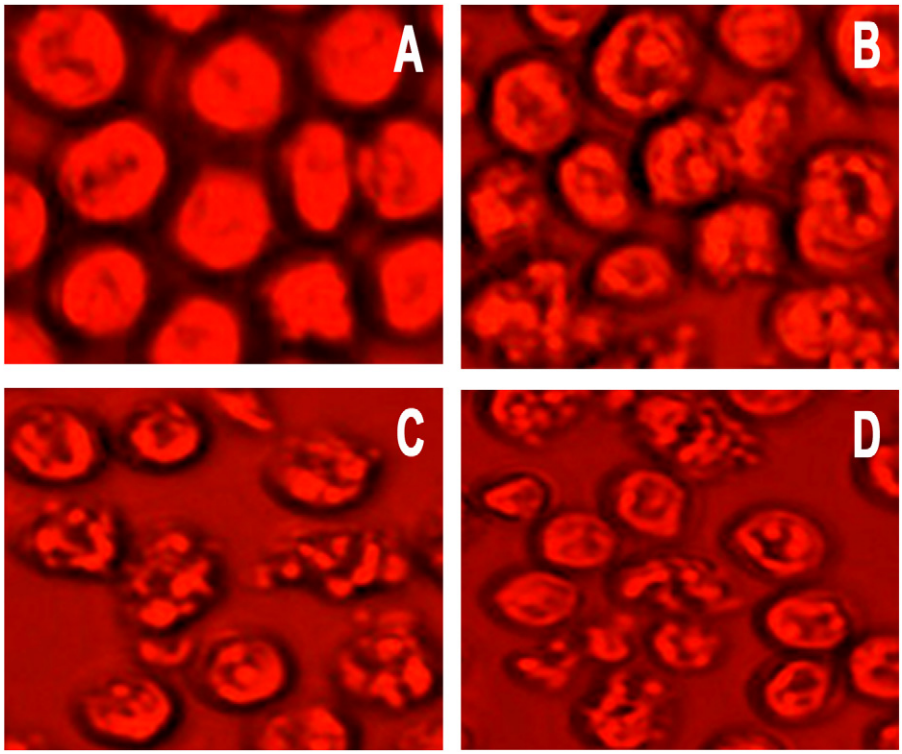

Fig. 3. A–D Nuclear fragmentation induced by resveratrol and its derivatives RA1 and RA2 at 10 μM for 48 h on U937 cell lines. Untreated cells are intact without any nuclear fragmentation whereas resveratrol and its derivatives RA1 and RA2 treated cells are showing characteristic nuclear fragmentation.

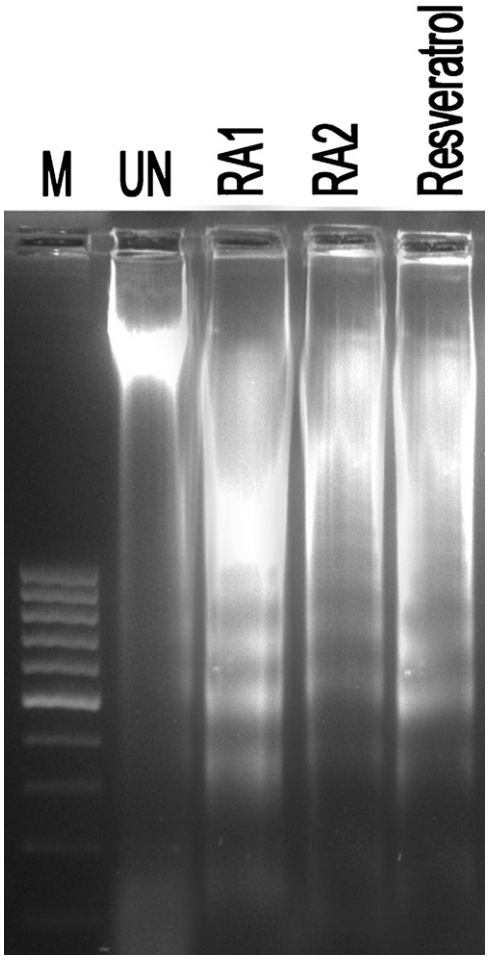

Fig. 4. DNA electrophoresis of resveratrol and its derivatives RA1 and RA2 treated U937 cells. U937 cells were cultured in the presence or absence of 10 μM resveratrol and its derivatives for 24 h.

controls. Both the resveratrol analogue treated cells showed prominent and characteristic fragments of DNA than resveratrol (Fig. 4). The pattern of ladder formation by resveratrol and its derivatives RA1 and RA2 supports, the mode of cell death in treated U937 cells is apoptosis. These hallmark features of morphological changes suggested that the treated resveratrol derivatives caused apoptosis of U937 cancer cells. This further supports the high potent action of resveratrol derivatives than that of resveratrol. This may be due to the increase in bioavailability of the resveratrol derivatives by the decrease of the free hydroxyl groups [46].

3.2.4. Resveratrol and its derivatives induces cleavage of PARP

Results obtained by PI staining and DNA fragmentation analysis showed that resveratrol and its derivatives RA1 and RA2, induced apoptosis in U937 cells. To confirm the mode of cell death as apoptosis, we performed PARP cleavage assay through Western blot analysis in resveratrol and its derivatives treated cells. U937 cells were treated with 10 μM concentration of resveratrol and its derivatives for 72 h and assayed their ability to cleave PARP protein. Treatment with resveratrol derivatives induced almost approximately 80% cleavage of PARP protein (Fig. 6A) whereas resveratrol was able to induce almost 50% of PARP cleavage (Fig. 6A). As discussed previously, by Wen and Walle [46] experiment it was found that capping of hydroxyl groups increases the half-life period of resveratrol. The results of the current study are in consistent with these results because in the resveratrol derivatives the hydroxyl groups are being capped.

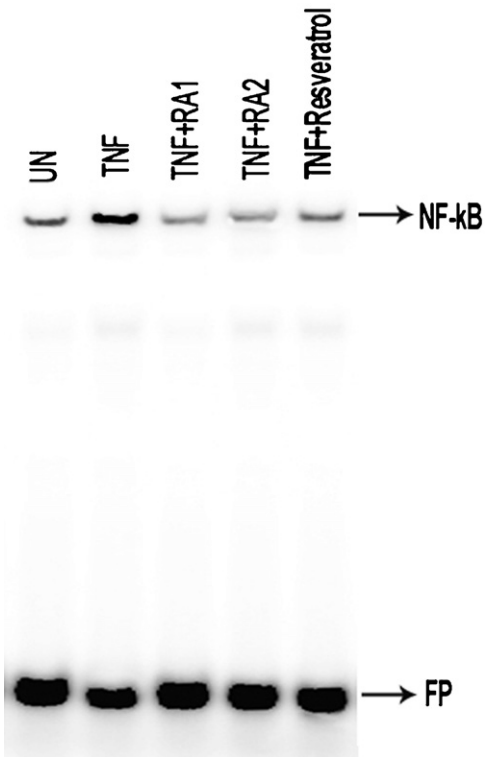

Fig. 5. Effect of resveratrol and its derivatives RA1 and RA2 on the activation of NF-kB. U937 cells were treated with resveratrol and its derivatives RA1 and RA2 (10 μM) for 48 h and then treated TNF for 1H. Nuclear extract were prepared and NF-kB binding was analyzed by EMSA using sequence-specific radiolabeled oligonucleotide.

3.2.5. Resveratrol and its derivatives decreases NF-kB binding to DNA in U937 cells

NF-kB expressing cells showed anti-apoptotic activity. U937 cells were pretreated with resveratrol and its derivatives for 48 h and then stimulated with TNF (0.1 nM) for 1 h. Cells were washed and nuclear extracts were prepared. 8 μg of nuclear extract proteins were assayed for NF-kB by EMSA. As shown in Fig. 5, TNF induced NF-kB activation potently and resveratrol and its derivatives inhibited this activation. Among the two resveratrol derivatives RA1 has shown higher rates of, suppression of NF-kB binding to DNA at 10 μM concentration. The inhibition of RA1 binding to DNA by NF-kB is higher than that of resveratrol (Fig. 5). It has been already shown that resveratrol suppress the DNA binding activity of NF-kB [13,48]. In this work, EMSA analysis clearly showed that resveratrol derivatives RA1 and RA2 suppressed the DNA binding ability of NF-kB (Fig. 5). The possible reasons that can be can be given for these results is resveratrol and its derivatives might have interfered in the translocation of NF-kB [13] or by binding to NF-kB these compounds might have interfered in the binding of NF-kB to DNA.

3.2.6. Resveratrol and its derivatives RA1 and RA2 enhances the expression of FasR, FasL and suppresses TNFα, TNFR, IL-8 and actin genes expression

As resveratrol and its derivatives were found to inhibit the binding of NF-kB to DNA and increases the cell death by apoptosis, the levels of expression of FasR, FasL, TNFα, TNFR, IL-8 and actin genes were determined by semi quantitative RT-PCR. Total RNA was isolated from U937 cells treated with resveratrol and its derivatives, RA1 and RA2 at 10 μM concentration for 72 h. This RNA was used for RT-PCR, followed by PCR using FASR, FASL, TNFα, TNFR, IL-8 and actin specific primers and analyzed by 1% agarose gel (Fig. 6B).

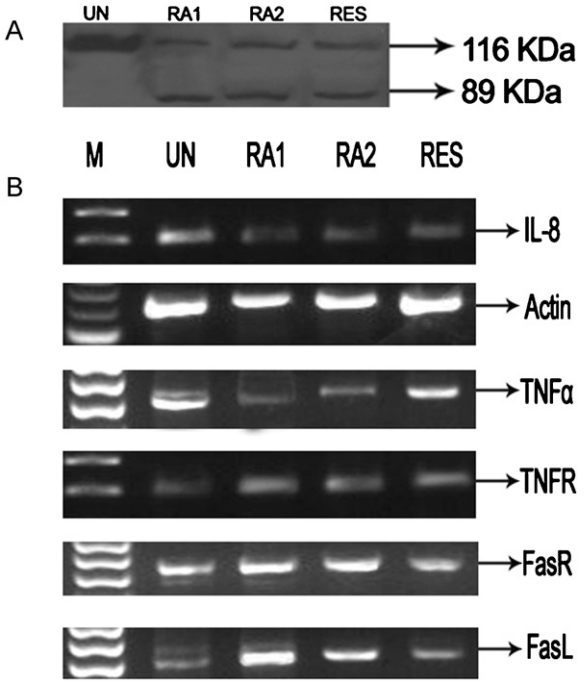

Fig. 6. (A) Effect of resveratrol and its derivatives RA1 and RA2 on PARP cleavage. U937 cells were treated with 10 μM concentration of resveratrol and its derivatives RA1 and RA2 for 72 h and PARP cleavage was determined by Western blot analysis. (B) Effect of resveratrol and its derivatives RA1 and RA2 on the amount of TNFα, TNFR, IL-8, actin FasL and FasR. U937 cells were treated with 10 μM concentration of resveratrol and its derivatives RA1 and RA2 for 72 h. The amounts of TNFα, TNFR, IL-8, actin FasR and FasL were detected by RT-PCR followed by PCR from total RNA.

Results showed that FasR and FasL genes got expressed in treated cells whereas TNFα, TNFR, IL-8 and actin genes were found to get suppressed in the treated cells. RA1 among the tested compounds is acting as a strong inhibitor of IL-8, TNFα, TNFR and actin whereas FasR, and FasL, were activated in presence of RA1. NF-kB enhances transcription of TNFα, TNFR, IL-8, actin and suppress the transcription of FasL and FasR genes by binding to promoter sites, so the capacity of resveratrol and its derivatives RA1 and RA2 to inhibit NF-kB activation would be expected to affect transcription of these genes [49].

3.3. *In silico evaluation*

3.3.1. *Molecular docking of resveratrol derivatives onto NF-kB*

The reported resveratrol derivatives RA1 and RA2 were showed better activity than parental molecule against cancerous cells and these were found to have OH-group substitutions [42–46]. However, the binding modes of resveratrol and its synthesized derivatives remain unknown. To study the possible binding modes of these compounds and to reveal the most essential amino acids involved in ligand recognition, molecular docking was performed.

The hundred docking conformations obtained for each compound were divided into groups according to 1.0 Å RMSD criterion by using the cluster module in ADT. Besides RMSD cluster analysis, AutoDock also uses binding free energy evaluation to find the best binding mode. Energy items calculated by AutoDock are characterized by intermolecular energy (consists of van der Walls energy, hydrogen bonding energy, desolvation energy and electrostatic energy), internal energy of ligand and tortional free energy. During all these interactions, the electrostatic interaction between ligands and receptor is most important, because in most cases it can decide the binding strength and the location of the ligand, while the hydrophobic interactions of some groups can affect the activity to a larger extent. The energy conformations of resveratrol and its derivatives RA1 and RA2 are listed in Table 2, and the interaction modes of the resveratrol and its derivatives are depicted in Fig. 7, where only the amino acid residues located within 10 Å of the ligands are displayed.

Docked conformations of the three compounds (resveratrol, RA1 and RA2) showed that all these molecules established interactions with the residues of NF-kB that are involved in DNA binding. RA1 among the three docked molecules (Fig. 7) formed more interactions with that of NF-kB, this might be due to ideal alignment of RA1 with NF-kB resulting in more inside with tight binding, in the NF-kB DNA binding domain. The residues that are involved in hydrogen bonding interactions with RA1 (Fig. 7B) are Arg^{35}(p65), Arg^{187}(p65), Tyr^{357}(p50), Lys^{444}(p50) and Lys^{575}(p50). In contrast to RA1, resveratrol (Fig. 7A) has shown less hydrogen bonding (four) interactions with NF-kB. Residues at the NF-kB site that form hydrogen bonding interactions with resveratrol are Arg^{33}(p65), Gln^{220}(p65), Lys^{572}(p50) and Gln^{606}(p50). Interestingly, RA2 (Fig. 7C) has also shown four hydrogen bonding interactions with Tyr^{36}(p65), Arg^{187}(p65), Arg^{354}(p50) and Lys^{541}(p50) at NF-kB binding domain. Along with hydrogen bonding all the molecules were shown to establish electrostatic interactions, hydrophobic interactions and aromatic interactions with NF-kB. Overall, we found that the binding affinity of ligands to NF-kB depends on physical interactions, such as hydrogen bonding, hydrophobic interactions and aromatic interactions and among all RA1 was able to establish strong interactions with NF-kB.

3.3.2. *Stability of the MD simulated complexes of NF-kB-resveratrol, NF-kB-RA1 and NF-kB-RA2*

To further assess the reliability of the docked NF-kB ligand structures, the conformation with the lowest interaction energy from the major cluster was refined by MD simulation. MD simulations were carried out for four systems: NF-kB structure in ligand-free form and the complexes of NF-kB-resveratrol, NF-kB-RA1 and NF-kB-RA2. The main purpose of this study is to elucidate the influence of resveratrol and its derivatives RA1 and RA2 on the overall structure of the NF-kB. In order to monitor the progress of NF-kB conformational changes and to check the stability of the protein during the simulations, we evaluated the RMSD of the positions for all backbone C-alpha atoms as a function of simulation time. As we can see in Fig. 8A, the overall structures were stable along the MD simulations. NF-kB alone has shown higher RMSD when compared with the complexes of NF-kB-resveratrol, NF-kB-RA1 and NF-kB-RA2 (Fig. 8A). In all simulated systems the RMSD of C-alpha atoms after a rapid increase showed a relative stability during overall MD simulation, achieving a plateau between 0.25 and 0.78 nm, suggesting that 10 ns of unrestrained simulation was sufficient for stabilizing NF-kB, NF-kB-resveratrol, NF-kB-RA1 and NF-kB-RA2 structures. Accordingly, the NF-kB-RA1 complex among all simulated complexes was shown to be more stable (Fig. 8A). All the simulated complexes (NF-kB-resveratrol, NF-kB-RA1, NF-kB-RA2) showed lesser RMSD values than that of NF-kB, this might be due to slight compacting process occurred on NF-kB due to the presence of ligands. The flexibilities of the residues in the protein were assessed by RMSF values from MD simulations of the trajectory, which reflects the flexibility of each atom residue in the molecule. Fig. 8B shows the plot per residue of the RMSF of NF-kB for complexes with resveratrol, RA1 and RA2. With the exception of the highly flexible termini, the complexes of NF-kB-resveratrol, NF-kB-RA1 and NF-kB-RA2 showed the suppression of mobility in several regions of the NF-kB protein, in particular the residues in the DNA binding domain (Fig. 8B). NF-kB-RA1 among the three simulated complexes has shown lesser RMS fluctuations. These results suggest a correlation between increased inhibition potency of the RA1 and its ability to stabilize the local protein fluctuations. The stability

Table 2
AutoDock results of Nf-kB with resveratrol and its derivatives RA1 and RA2.

Compound	Binding energy (kcal/mol)	Docked energy (kcal/mol)	RMSD (Å)	Cluster number	Estimated K_i (μM)
Resveratrol	−6.12	−6.01	0.8943	23	32.64
RA1	−8.02	−7.93	0.7698	40	1.322
RA2	−7.35	−6.70	0.8219	36	12.150

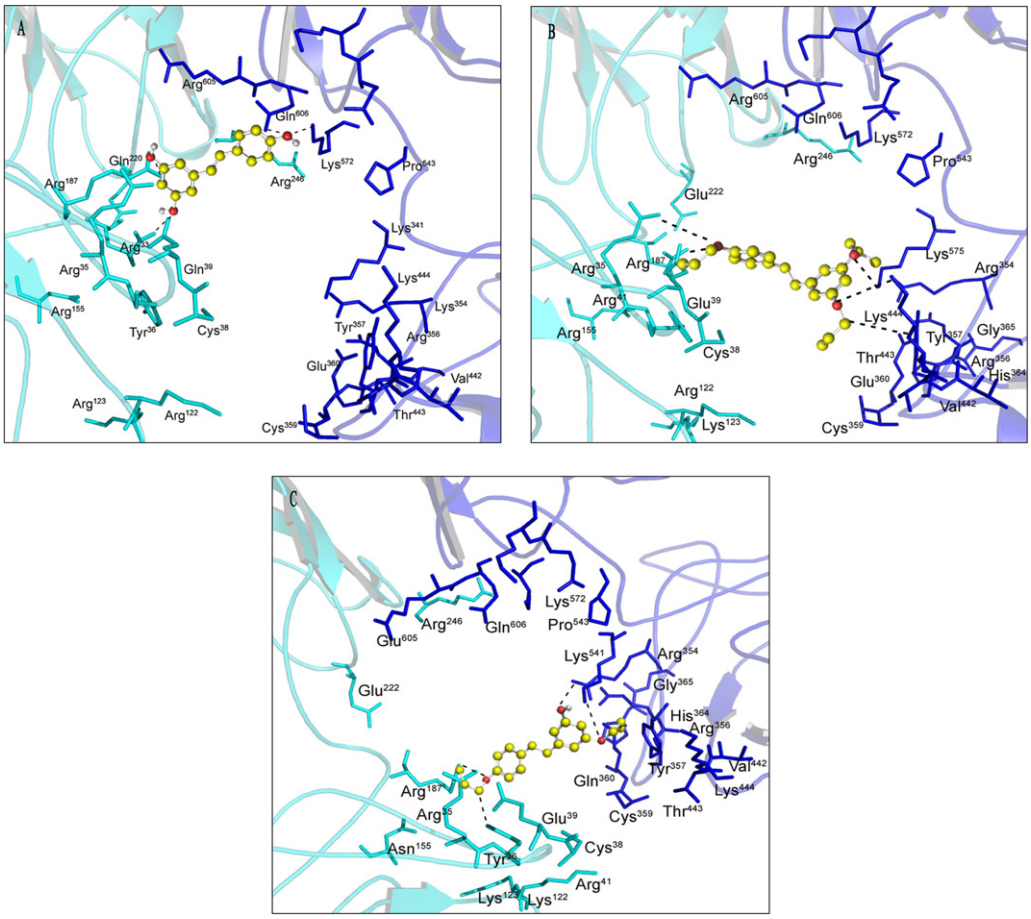

Fig. 7. Resveratrol and its derivatives RA1 and RA2 were docked with NF-kB using AutoDock 4.2. NF-kB is represented in cartoon conformation and p65 subunit is represented in cyan and p50 is in blue. Residues interacting with ligands are given line conformation. Resveratrol and its derivatives RA1 and RA2 were given atom type ball and stick representation. (For interpretation of the references to color in this figure legend, the reader is referred to the web version of the article.)

of the simulations can be viewed by analyzing the total energy as a function of time. The total energy (kJ/mol) of the protein with resveratrol and its derivatives RA1 and RA2 is relatively lower when compared with that of protein alone throughout the simulation (Table 3).

The specificity and affinity between NF-kB and its inhibitor depends on the direction of hydrogen bonds and ionic interactions, as well as on shape complementarities of the contact surfaces of both ligand and the protein. To verify the complexes of NF-kB-resveratrol, NF-kB-RA1 and NF-kB-RA2 structural associations throughout the MD simulation, the total number hydrogen bonds between NF-kB and ligands were measured over the period of simulation (Fig. 8C). The time dependent hydrogen bonding pattern growth curve apparently showed that the binding partners maintained dynamically and attained their close contact in a polar environment. All the original hydrogen bonds were retained for resveratrol, RA1 and RA2 in addition to this few new hydrogen bonds are generated for all the molecules. RA1 among all had shown a maximum of five hydrogen bonds whereas resveratrol and RA2 have shown four hydrogen bonds. Newly formed interactions between ligands were also established between residues of DNA binding domain of NF-kB. The possible reason for this is all the three molecules were able to establish stable interactions with NF-kB at its DNA binding domain during dynamic simulations.

Table 3
Time averaged energies obtained for NF-kB and its complexes with resveratrol and its derivatives RA1 and RA2.

Complex	Average total energy (kcal/mol)	Average kinetic energy (kcal/mol)	Average potential energy (kcal/mol)
NF-kB	−990,382	−211,438	−1,201,820
NF-kB-resveratrol	−969,214	−212,556	−1,181,770
NF-kB-RA1	−966,675	−212,520	−1,178,195
NF-kB-RA2	−967,588	−211,536	−1,181,324

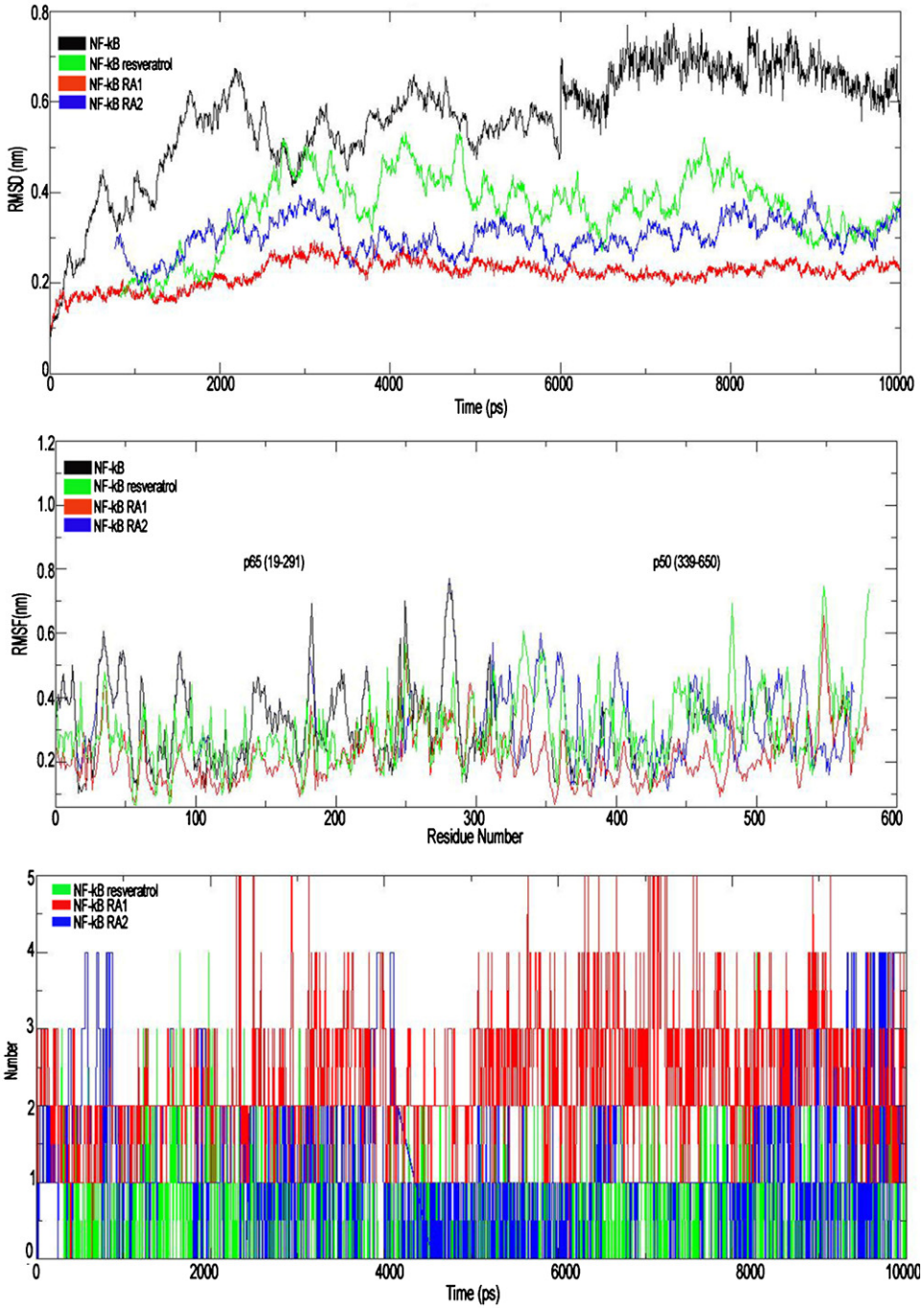

Fig. 8. (A) C-alpha RMSDs of NF-kB, NF-kB-resveratrol, NF-kB-RA1 and NF-kB-RA2. (B) RMSF values NF-kB, NF-kB-resveratrol NF-kB-RA1 and NF-kB-RA2 generated by Gromacs. (C) Hydrogen bonds generated by the simulated complexes NF-kB-resveratrol, NF-kB-RA1 and NF-kB-RA2.

Our dynamic study showed that resveratrol and its derivatives can steadily anchor to NF-kB to exert an inhibition effect of binding to DNA.

3.3.3. *Docking of stabilized complexes of NF-kB with DNA*

To unravel the molecular mechanism of suppression of DNA binding by NF-kB complexes of resveratrol and its derivatives (RA1, RA2), docking was performed. Four independent docking were performed, docking of free NF-kB with DNA, docking NF-kB-resveratrol complex with DNA, docking of NF-kB-RA1 complex with DNA and docking of NF-kB-RA2 complex with DNA. Docking result of NF-kB-resveratrol complex (Fig. 9) revealed that binding of resveratrol to the some of the residues involved in the interaction of DNA (Fig. 9) has changed the topology of the DNA binding domain (Fig. 9). NF-kB-RA1 complex and NF-kB-RA2 complex when docked with DNA has shown (Figs. 10 and 11) that these two ligands were also established interactions with residues of DNA binding domain of NF-kB and changed the topological conformation of the NF-kB at the interaction site of DNA. Energy total obtained for NF-kB alone docked with DNA (−3005.72 kcal/mol) is higher when compared to complexes of NF-kB-resveratrol (−728.25 kcal/mol), NF-kB-RA1 (−687.86 kcal/mol) and NF-kB-RA2 (−714.95 kcal/mol). RMSD superposition of NF-kB-resveratrol-DNA (0.9652 Å), NF-kB-RA1-DNA (1.3269 Å) and NF-kB-RA2-DNA (1.0285 Å) complexes

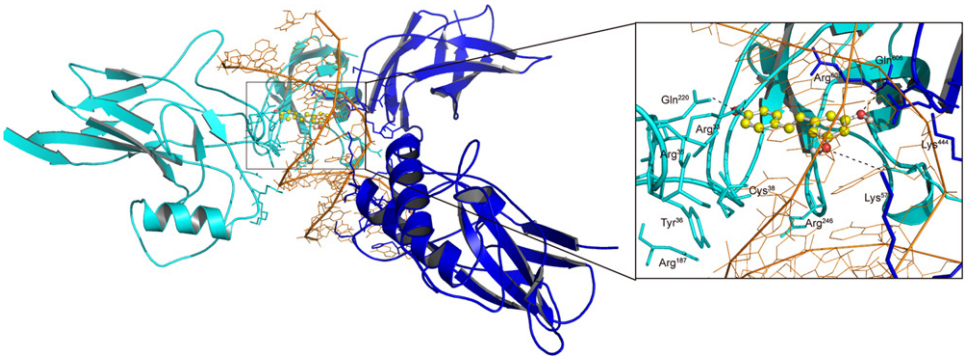

Fig. 9. NF-kB-resveratrol complex was docked with DNA using HEX. NF-kB is represented in cartoon conformation and p65 subunit is represented in cyan color whereas p50 is given blue. Residues at DNA binding domain are represented in sticks. Resveratrol is represented in atom type ball and stick conformation. DNA is represented in orange color. (For interpretation of the references to color in this figure legend, the reader is referred to the web version of the article.)

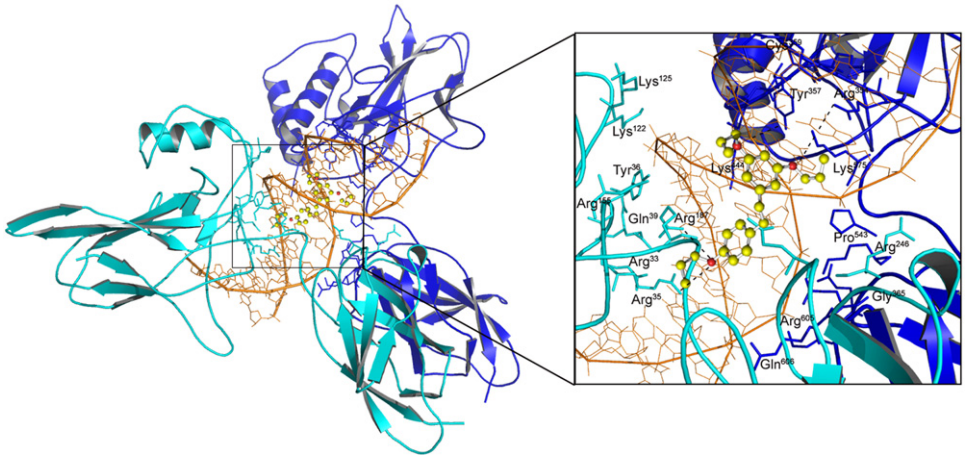

Fig. 10. NF-kB-RA1 complex was docked with DNA using HEX. NF-kB is represented in cartoon conformation and p65 is represented in cyan color whereas p50 is given blue. Residues at DNA binding domain are represented in sticks. RA1 is represented in atom type ball and stick conformation. DNA is represented in orange color.

onto NF-kB-DNA complex showed that NF-kB RA1 DNA (1.3269 Å) complex has displayed higher RMSD superposition values. This can be due to higher degree of change in orientation of residues that interacting with RA1 at DNA binding domain of NF-kB. This might be the reason for interference of NF-kB binding to DNA and also for more potent action of RA1 among the two derivatives.

In this study, resveratrol, a natural polyphenol, and its derivatives RA1 and RA2, were chemically synthesized in order to investigate their anti-proliferation effects. Examination of the relation of the structures to anti-proliferation activity through in vitro and in silico analyses suggests that the allyl groups added to RA1 by substituting the three hydroxyl groups has shown more potent

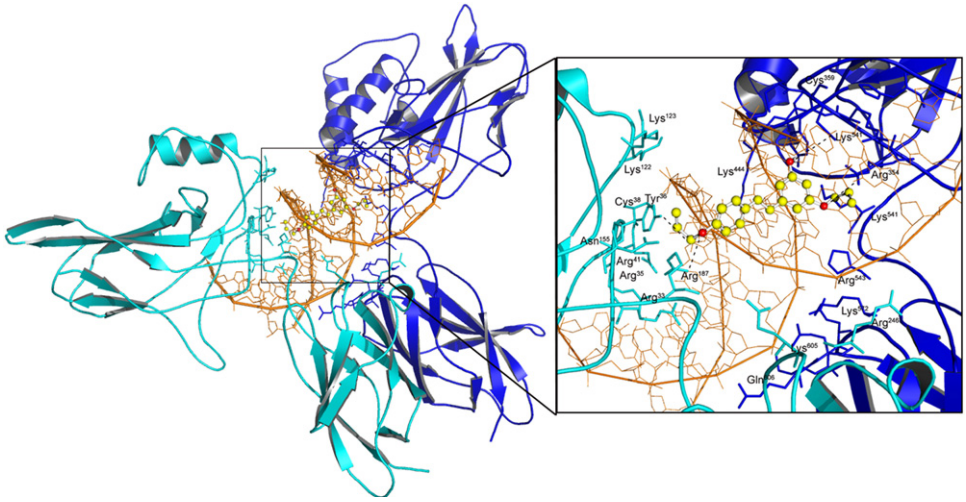

Fig. 11. NF-kB-RA2 complex was docked with DNA using HEX. NF-kB is represented in cartoon conformation and p65 is represented in cyan color whereas p50 is given blue. Residues at DNA binding domain are represented in sticks. RA1 is represented in atom type ball and stick conformation. DNA is represented in orange color. (For interpretation of the references to color in this figure legend, the reader is referred to the web version of the article.)

activity. This might be due to increase in the half-life period and bioavailability of the compound. Whereas when allyl groups are added to two of the three hydroxyl groups (3,4′-hydroxyl) smaller deduction in anti-proliferation activity was seen [48]. In the two synthesized resveratrol derivatives RA1 and RA2 the hydroxyl groups are capped, this might be reason for the enhancement of their bioavailability and half-life [46,47]. It is generally accepted that capping of hydroxyl groups prevents glucuronidation in liver and intestinal cells and may enhances bioavailability and half-life in in vivo [46,47]. The decrease in anti-proliferative activities of resveratrol than its synthesized derivatives is due to the presence of free hydroxyl groups. It has been known that compounds possessing free hydroxyl groups may present reduced pharmacological and antiproliferative activities, due to rapid excretion [46,47]. A recent study underlined the importance of methoxylation in transstilbenes in increasing the toxicity toward *Caenorhabditis elegans* [50]. The order of potency of the synthesized resveratrol analogues is RA1 > RA2 > resveratrol. The results obtained in this study showed that the synthesized resveratrol derivatives possess more potent apoptosis-inducing activity than resveratrol and these compounds are of great interest for further investigation.

Conflict of interest

The authors declare that they have no conflict of interest in publishing this article.

Acknowledgements

This study was supported by the Department of Biotechnology (DBT), Bioinformatics Infrastructure Facility (BIF) (F.NO BT/BI/25/2001/2006). We are grateful to Dr. Sunil Kumar Manna, Scientist, CDFD and Dr. J. Gowrishankar, Director, CDFD, Hyderabad for their help and support in in vitro studies. The authors Ms. M. Chaitanya and B. Babajan want to thank CSIR for providing SRF fellowship. Mr. P. Madhusudana thanks to ICMR for SRF.

Appendix A. Supplementary data

Supplementary data associated with this article can be found, in the online version, at http://dx.doi.org/10.1016/j.jmgm.2013.01.005.

References

[1] G. Block, B. Patterson, A. Subar, Fruit, vegetables, and cancer prevention: a review of the epidemiological evidence, Nutrition and Cancer 18 (1992) 1–29.
[2] W.C. Willett, Diet and health: what should we eat, Science 264 (1994) 532–537.
[3] A.B. Miller, Diet and cancer: a review, Rev. Oncol. 3 (1990) 87–95.
[4] L.W. Wattenberg, Inhibition of carcinogenesis by minor dietary constituents, Cancer Research 52 (1992) 2085–2091.
[5] F.B. Hu, M.J. Stampfer, J.E. Manson, E. Rimm, G.A. Colditz, B.A. Rosner, C.H. Hennekens, W.C. Willett, Dietary fat intake and the risk of coronary heart disease in women, New England Journal of Medicine 337 (1997) 1491–1499.
[6] S.M. Kuo, Dietary flavonoid and cancer prevention: evidence and potential mechanism, Critical Reviews in Oncogenesis 8 (1997) 47–69.
[7] Y. Surh, Molecular mechanisms of chemopreventive effects of selected dietary and medicinal phenolic substances, Mutation Research 428 (1999) 305–327.
[8] Y.J. Surh, Cancer chemoprevention with dietary phytochemicals, Nature Reviews Cancer 3 (2003) 768–780.
[9] B.B. Aggarwal, A. Bhardwaj, R.S. Aggarwal, N.P. Seeram, S. Shishodia, Y. Takada, Role of resveratrol in prevention and therapy of cancer: preclinical and clinical studies, Anticancer Research 24 (2004) 2783–2840.
[10] M. Jang, L. Cai, G.O. Udeani, K.V. Slowing, C.F. Thomas, C.W. Beecher, H.H. Fong, N.R. Farnsworth, A.D. Kinghorn, R.G. Mehta, R.C. Moon, J.M. Pezzuto, Cancer chemopreventive activity of resveratrol, a natural product derived from grapes, Science 275 (1997) 218–220.
[11] A.M. Bode, Z. Dong, Signal transduction pathways: targets for chemoprevention of skin cancer, Lancet Oncology 1 (2000) 181–188.
[12] Z. Dong, Molecular mechanism of the chemopreventive effect of resveratrol, Mutation Research 523–524 (2003) 145–150.
[13] S.K. Manna, A. Mukhopadhyay, B.B. Aggarwal, Resveratrol suppresses TNF-induced activation of nuclear transcription factors NF-kappa B, activator protein-1 and apoptosis: potential role of reactive oxygen intermediates and lipid peroxidation, Journal of Immunology 164 (2000) 6509–6519.
[14] S.H. Tsai, S.Y. Lin-Shiau, J.K. Lin, Suppression of nitric oxide synthase and the down-regulation of the activation of NFkappaB in macrophages by resveratrol, British Journal of Pharmacology 126 (1999) 673–680.
[15] C. Huang, W.Y. Ma, A. Goranson, Z. Dong, Resveratrol suppresses cell transformation and induces apoptosis through a p53-dependent pathway, Carcinogenesis (London) 20 (1999) 237–242.
[16] N. Carbo, P. Costelli, F.M. Baccino, F.J. Lopez-Soriano, J.M. Argiles, Resveratrol a natural product present in wine, decreases tumour growth in a rat tumour model, Biochemical and Biophysical Research Communications 254 (1999) 739–743.
[17] T.C. Hsieh, J.M. Wu, Differential effects on growth, cell cycle arrest, and induction of apoptosis by resveratrol in human prostate cancer cell lines, Experimental Cell Research 249 (1999) 109–115.
[18] C.A. Lipinski, F. Lombardo, W. Dominy, P.J. Feeney, Experimental and computational approaches to estimate solubility and permeability in drug discovery and development settings, Advanced Drug Delivery Reviews 46 (2001) 3–26.
[19] P.B. Raghavendra, Y. Sreenivasan, G.T. Ramesh, S.K. Manna, Cardiac glycoside induces cell death via FasL activating calcineurin and NF-AT, but apoptosis initially proceeds through activation of caspases, Apoptosis 12 (2007) 307–318.
[20] E. Nutku, Q. Zhuang, A. Soussi-Gounni, F. Aris, B.D. Mazer, Q. Hamid, Functional expression of IL-12 receptor by human eosinophils: IL-12 promotes eosinophil apoptosis, Journal of Immunology 67 (2001) 1039–1046.
[21] D. Baskic, S. Popovic, P. Ristic, N.N. Arsenilevic, Analysis of cycloheximide-induced apoptosis in human leukocytes: fluorescence microscopy using annexin V/propidium iodide versus acridine orange/ethidium bromide, Cell Biology International 30 (2006) 924–932.
[22] J. Rudner, C.E. Ruiner, R. Handrick, H.J. Eibi, C. Belka, V. Jendrossek, The Akt-inhibitor Erufosine induced apoptotic cell death in prostate cancer cells and increases the short term effects of ionizing radiation, Radiation Oncology 16 (2010) 108.
[23] S.K. Manna, S. Sarkar, J. Barr, K. Wise, E.V. Barrera, O. Jeielowo, A.C. Rice-Ficht, G.T. Ramesh, Single-walled carbon nanotube induces oxidative stress and activates nuclear transcription factor-kappa B in human keratinocytes, Nano Letters 5 (2005) 1676–1684.
[24] J.C. Stroud, A. Oltman, A. Han, D.L. Bates, L. Chen, Structural basis of HIV-1 activation by NF-kappaB – a higher order complex of p50:RelA bound to the HIV-1 LTR, Journal of Molecular Biology 393 (2009) 98–112.
[25] B. Hess, C. Kutzner, D. van der Spoel, E. Lindahl, GROMACS 4: algorithms for highly efficient, load-balanced, and scalable molecular simulation, Journal of Chemical Theory and Computation 4 (2008) 435–447.
[26] W.F. van Gunsteren, S.R. Billeter, A.A. Eising, P.H. Hunenberger, P. Kruger, A.E. Mark, W.R.P. Scott, I.G. Tironi, Biomolecular Simulation: The Gromos 96 Manual and User Guide, Hochschulverlag AG an der Zurich, Zurich, Switzerland, 1996.
[27] H.J.C. Berendsen, J.P.M. Postma, W.F. van Gunsteren, J. Hermans, Interaction models for water in relation to protein hydration, in: B. Pullman (Ed.), Inter Molecular Forces, D Reidel Publishing Company, Dordrecht, 1981, pp. 331–342.
[28] H.J.C. Berendsen, J.P.M. Postma, W.F. van Gunsteren, A. Dinola, J.R. Haak, Molecular dynamic with coupling to an external bath, Journal of Chemical Physics 81 (1984) 3684–3690.
[29] B. Hess, H. Bekker, H.J.C. Berendsen, J.G.E.M. Fraaije, LINCS: a linear constraint solver for molecular simulations, Journal of Computational Chemistry 18 (1997) 1463–1472.
[30] D. York, W. Yang, The fast Fourier Poisson method for calculating EWALD sums, Journal of Chemical Physics 101 (1994) 3298–3300.
[31] D.M.F. van Aalten, R. Bywater, J.B.C. Findlay, M. Hendlich, R.W.W. Hooft, G. Vriend, PRODRG, a program for generating molecular topologies and unique molecular descriptors from coordinates of small molecules, Journal of Computer-Aided Molecular Design 10 (1996) 255–262.
[32] G.M. Morris, D.S. Goodsell, R.S. Halliday, R. Huey, W.E. Hart, R.K. Belew, A.J. Olson, AutoDock, Version 4.0.1, The Scripps Research Institute, La Jolla, CA, USA, 2007.
[33] M.F. Sanner, R. Huey, S. Dallakyan, S. Karnati, W. Lindstrom, G.M. Morris, B. Norledge, A. Omelchenko, D. Stoffler, G. Vareille, AutoDockTools, Version 1.4.5, The Scripps Research Institute, La Jolla, CA, USA, 2007.
[34] R. Huey, G.M. Morris, A.J. Olson, D.S. Goodsell, A semiempirical free energy force field with charge-based desolvation, Journal of Computational Chemistry 28 (2007) 1145–1152.
[35] G.M. Morris, D.S. Goodsell, R.S. Halliday, R. Huey, W.E. Hart, R.K. Belew, A.J. Olson, Automated docking using a Lamarckian genetic algorithm and an empirical binding free energy function, Journal of Computational Chemistry 19 (1998) 1639–1662.
[36] G.M. Morris, D.S. Goodsell, R. Huey, A.J. Olson, Distributed automated docking of flexible ligands to proteins: parallel applications of AutoDock 2.4, Journal of Computer-Aided Molecular Design 10 (1996) 293–304.
[37] D.S. Goodsell, A.J. Olson, Automated docking of substrates to proteins by simulated annealing, Proteins 8 (1990) 195–202.
[38] S. Miyamoto, P.A. Kollman, Settle: an analytical version of the SHAKE and RATTLE algorithm for rigid water models, Journal of Computational Chemistry 13 (1992) 952–962.
[39] H. Schreiber, O. Steinhauser, Taming cut-off induced artifacts in molecular dynamics studies of solvated polypeptides. The reaction field method, Journal of Molecular Biology 228 (1992) 909–923.

[40] P.E. Smith, W.F. van Gunsteren, Consistent dielectric properties of the simple point charge and extended simple point charge water models at 277 and 300k, Journal of Chemical Physics 100 (1994) 3169–3174.
[41] W. Humphrey, A. Dalke, K. Schulten, VMD: visual molecular dynamics, Journal of Molecular Graphics 14 (1996) 33–38, 27–28.
[42] W.L. DeLano, S. Bromberg, PyMOL User's Guide, DeLano Scientific LLC, San Francisco, 2004.
[43] G. Macindoe, L. Mavridis, V. Venkatraman, M.D. Devignes, D.W. Ritchie, HexServer: an FFT-based protein docking server powered by graphics processors, Nucleic Acids Research 38 (2010) 445–449.
[44] F. Minutolo, G. Sala, A. Bagnacani, S. Bertini, I. Carboni, G. Placanica, G. Prota, S. Rapposelli, N. Sacchi, M. Macchia, R. Ghidoni, Synthesis of a resveratrol analogue with high ceramide-mediated proapoptotic activity on human breast cancer cells, Journal of Medicinal Chemistry 48 (2005) 6783–6786.
[45] D. Simoni, M. Roberti, F.P. Invidiata, E. Aiello, S. Aiello, P. Marchetti, R. Baruchello, M. Eleopra, A. Di Cristina, S. Grimaudo, N. Gebbia, L. Crosta, F. Dieli, M. Tolomeo, Stilbene-based anticancer agents: resveratrol analogues active toward HL60 leukemic cells with a non-specific phase mechanism, Bioorganic and Medicinal Chemistry Letters 16 (2006) 3245–3248.
[46] X. Wen, T. Walle, Methylated flavonoids have greatly improved intestinal absorption and metabolic stability, Drug Metabolism and Disposition: The Biological Fate of Chemicals 34 (2006) 1786–1792.
[47] T. Walle, Absorption and metabolism of flavonoids, Free Radical Biology and Medicine 36 (2004) 829–837.
[48] M.H. McNary, A.S. Baldwin Jr., Chemopreventive properties of trans-resveratrol are associated with inhibition of activation of the IkB kinase, Cancer Research 60 (2000) 3477–3483.
[49] S. Huang, L. Zhao, K. Kim, D.S. Lee, D.H. Hwang, Inhibition of Nod2 signaling and target gene expression by curcumin, Molecular Pharmacology 74 (2008) 274–281.
[50] M.A. Wilson, A.M. Rimando, C.A. Wolkow, Methoxylation enhances stilbene bioactivity in *Caenorhabditis elegans*, BMC Pharmacology 8 (2008) 15–25.